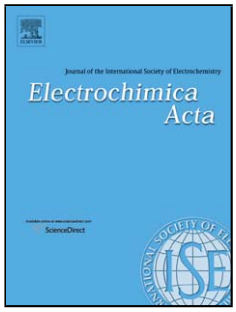

Title: Influence of magnetic field on hydrogen reduction and co-reduction in the $Cu/CuSO_4$ system

Authors: Dámaris Fernández, Zhu Diao, Peter Dunne, J.M.D. Coey

PII: S0013-4686(10)01056-X
DOI: doi:10.1016/j.electacta.2010.08.004
Reference: EA 16084

To appear in: *Electrochimica Acta*

Received date: 13-1-2010
Revised date: 2-8-2010
Accepted date: 3-8-2010

Please cite this article as: D. Fernández, Z. Diao, P. Dunne, J.M.D. Coey, Influence of magnetic field on hydrogen reduction and co-reduction in the $Cu/CuSO_4$ system, *Electrochimica Acta* (2010), doi:10.1016/j.electacta.2010.08.004

Influence of magnetic field on hydrogen reduction and co-reduction in the Cu/$CuSO_4$ system

Authors:

Dámaris Fernández*, Zhu Diao, Peter Dunne, JMD Coey

School of Physics and CRANN, Trinity College, Dublin 2, Ireland.

Keywords: magnetoelectrodeposition, electrochemical noise, hydrogen evolution reaction (HER), copper, growth.

Abstract

The effects of an applied magnetic field of up to 5 T on hydrogen evolution and cathodic overpotential were studied for H_2SO_4 and an acidic Cu/$CuSO_4$ system. Cyclic voltammetry, potentiostatic and galvanostatic deposition as well as electrochemical noise measurements were used. The magnetic field simultaneously increases the rate of hydrogen evolution and modifies the hydrogen bubble size. The periodicity of bubble release from a microelectrode is strongly influenced by the field, which may change the characteristic frequency or make it aperiodic, depending on the field orientation relative to buoyancy. The magnetic field stabilizes a bubble growing on a microelectrode, especially at high current densities. For example, bubble volume increases by a factor four in 1.5 T when the Lorentz force acts downwards. The noise spectra around 1 kHz are characteristic of a coalescence phenomenon. Hydrogen co-reduction with copper was studied by scanning electron microscopy and the current efficiency was measured with a quartz crystal microbalance; at -1.0 V it decreases from 95 % to 75 % in a field of 1.5 T. Bubble release is no longer periodic, but the noise spectrum has a characteristic shape depending on whether the current density is greater than, equal to or less than the diffusion-limited copper current. The field reduces the roughness of the copper deposit, but the current efficiency can be maximized by controlling the system galvanostatically, which allows a high copper deposition rate at overpotential lower than 0.5 V in the applied field, with smooth deposit quality.

1. Introduction

The hydrogen evolution reaction (HER) occurs during copper electrodeposition in conditions of high cathodic overpotential η with respect to the Cu^{2+}/Cu^{0} couple, the exact value depending on the system's pH. Hydrogen reduction is usually to be avoided during copper electroplating, because it has a detrimental effect on deposit quality; gas formation on the surface implies its partial occlusion, impeding the reduction and deposition of cupric ions in the occluded zones, which reduces the current efficiency. However, hydrogen evolution is also interesting for energy storage and fuel cell technologies, and new developments regarding hydrogen production during electrodeposition have been envisaged, such as the use of hydrogen bubbles as dynamic templates for conducting foams [1-4]

When copper films are obtained by electrodeposition at high overpotential, two factors concur to give rough surfaces; on the one hand diffusion limits mass transport in the system when the overpotential is higher than approximately -400 mV. Dendritic growth predominates as a consequence, leading to rough films. On the other hand, gas formation at the growing surface leaves marks such as pores where a bubble grew.

It is known that when a magnetic field is applied during mass transport limited electrochemical reactions, their rates increase and the morphology of deposit is improved. These changes are due to magnetohydrodynamic (MHD) effects of the Lorentz force

$$\boldsymbol{F}_{\mathrm{L}} = \boldsymbol{j} \times \boldsymbol{B} \qquad (1)$$

where $\boldsymbol{j}$ is the current density [A cm^{-2}], $\boldsymbol{B}$ is the applied magnetic field [T], and $\boldsymbol{F}_{\mathrm{L}}$ is the local force density which causes magnetoconvection. This makes magnetoelectrodeposition an attractive technique due to the possibility of working at higher current densities [5-7]. However, in many electroplating systems such as copper, the hydrogen co-reduction reaction occurs at higher overpotentials. According to the literature, H_2 evolution can also be affected by the field. In the case of the Cu system, Hinds et al [7] reported that the typical inflection due to hydrogen evolution at the highest part of the cathodic branch was somehow suppressed by a magnetic field. For the nickel system, Devos et al [8] showed, by inspection of marks in the deposit, that hydrogen bubble formation was affected by magnetic field-induced convection, whereas Bund and Ispas [9] observed increments in

hydrogen current and a reduction of plating efficiency and surface quality for nickel due to the influence of field on the hydrogen evolution reaction. In the cobalt system, Uhlemann et al [10] measured the local pH value directly at the surface, determining that magnetic fields increase hydrogen reduction currents and enhance ion replenishment at the electrode. This was accompanied by improvements in deposit quality. Using a quartz crystal microbalance, they confirmed the enhancement of the hydrogen current [11]. Koza and coworkers found that, during deposition of CoFe alloys, a field applied perpendicular to the electrode surface promotes hydrogen desorption, which they attributed to the twisting action of the Lorentz force around the growing hydrogen bubbles [12].

Matsushima et al [13] reported that magnetic fields tend to reduce supersaturation of hydrogen in solution and enhance mass transport of the dissolved H_2. Koza et al [14, 15] have shown that desorption of hydrogen from a horizontal electrode in the form of numerous small bubbles is enhanced in the cobalt system when a magnetic field is applied.

Electrochemical noise measurements are a good way to investigate bubbling systems. In particular, low-frequency noise varying with frequency f as $1/f^2$, was reported by Gabrielli and coworkers [16-19]. A model, treating bubbles departures as a sequence of random events, was used to explain the observed spectrum, and could reproduce some of these features [19]. Steyer et al explained that the $1/f^2$ noise spectrum is characteristic of a coalescence phenomenon [20], where an assembly of gas droplets grow on a substrate and coalesce when they touch according to the mass conservation rule. A recent report by Diao et al on the hydrolysis of water [21] showed that a magnetic field could either increase or decrease the hydrogen bubble size, and that this was associated with characteristic electrical noise spectra, measured at constant current. An earlier study using noise analysis for hydrogen evolution from copper microelectrodes immersed in H_2SO_4 solutions focussed on the kinetics of the reaction [22]. To our knowledge, this technique has not been used to describe hydrogen bubble release in the copper system, and there has been no quantitative or morphological analysis regarding magnetic field effects on the hydrogen evolution.

Here, we address magnetic field effects on hydrogen reduction and co-reduction with copper, on a microscopic scale. We characterize the magnetic field effect on the hydrogen evolution when protons are cathodically reduced on a copper substrate, both in

the presence and absence of cupric ions in acid sulphate electrolytes. Potentiodynamic, potentiostatic and galvanostatic techniques are used. We focus on the electrochemical noise spectra, but the electrochemical quartz crystal microbalance (EQCM) was also used to observe the changes in current efficiency during copper plating, and the deposit morphology has been characterized by scanning electron microscopy in order to gain a visual impression of the magnetic field effect on hydrogen bubble growth.

2. Experimental method

2.1 *Magnetoelectrochemical cell:* The system studied is a copper substrate in contact with an acid sulphate electrolyte containing 1.2 M H_2SO_4, either copper-free or containing 0.3 M $CuSO_4$. A 100 mL, round-bottom cylindrical cell was used. Three types of working electrodes were used: polished copper disks, ultrasmooth sputtered copper on silicon and copper microelectrodes. The polished disks were made from high purity rod (+99.999%) and had an exposed area of diameter 5.4 mm. The sputtered substrates had a root mean square roughness of less than 1 nm, and the cathodic area was defined as a 5 mm diameter circle by using a Kapton tape mask. The microelectrodes were made from 130 μm copper wire (+99.99%), inserted in Teflon tubes and filled with resin. The tubes were ground and polished transversally to their axis so that a circular copper microdisks was exposed. All the working electrodes in the experiments discussed here were arranged vertically, with vertical or horizontal magnetic fields applied parallel to the surface. The counter-electrode was Pt wire or sheet with an area of ~ 600 mm^2, and a pseudo-reference electrode was made from Cu wire. This was found to be as stable as a saturated $Cu/CuSO_4$ reference electrode, with the advantage that it is so small that it does not perturb convection in front of the cathode. This is important as we are interested in convective effects of the magnetic field. Cathodic potentials here are quoted as overpotential (η), and they correspond to negative voltages with respect to the Cu^{2+}/Cu^0 couple. The current density j is defined as the ratio of the applied current to the surface area of the polished copper cathode. We use a sign convention where j is a current of positive charge flowing towards the cathode, which corresponds to the definition of the Lorentz force density in Eq. (1).

2.2 *Equipment:* Uniform horizontal magnetic fields up to 1.5 T were produced by an electromagnet with 200 mm pole faces, while uniform vertical fields of up to 5 T were generated in the 110 mm vertical bore of a cryogen-free superconducting magnet where the field was parallel to the bore axis. The homogeneity of these fields over the cell volume was better than 1%. An EG&G potentiostat/galvanostat model EG270 was used to measure the electrochemical response.

The morphology of the deposits was examined by scanning electron microscopy (SEM); in some cases a focused ion beam (FIB) was used to section samples in order to view the deposit profile. Either a Zeiss-Ultra SEM system or a FEI Strata DB 235 Dual beam FIB/SEM instrument was used. In some cases deposit roughness was measured by atomic force microscopy (AFM) using a Nanoscope III (Veeco).

The electrochemical noise study was carried out by feeding the analogue output of the potentiostat directly to a SR560 voltage preamplifier (Stanford Research Systems), serving as an anti-aliasing filter. A computer controlled by a Labview program with a DAQ card (National Instrument M6250) working at a sampling frequency up to 100 kHz was used to record time sequences,. The noise spectrum was obtained by Fourier transforming the digitised time-domain signal.

The electrochemical quartz crystal microbalance (EQCM) consists of a Hameg HM8122 Counter Timer, a Maxtech Ltd. resonator model PL-70 and Testbourne Ltd. 5 MHz gold plated 25 mm diameter quartz crystals. The frequency response was monitored using another Labview program.

3. Results

3.1 *Hydrogen reduction.*

3.1.1 *Electrochemical characterization:* In order to understand the magnetic field effect on the copper/hydrogen system, it is useful to begin by examining the effects on the hydrogen reaction alone; tests were performed for the 1.2 M H_2SO_4 electrolyte without any copper content and results were obtained for both the 5.4 mm electrode and the microelectrode with different orientations of current and applied field. Figure 1 (a) shows the cyclic voltammograms for a 5.4 mm vertical electrode under vertical fields from 0 to 5 T. For this configuration the resulting *Lorentz force acts sideways*, across the surface of the

vertical electrode, as the inset shows. It can be seen that the field increases the hydrogen current, but most of the increase is achieved in fields of up to 1 T.

Figure 2 shows some current-time sequences when η = -1.0 V was applied in the same configuration. The current increases, in accord with the cyclic voltammogram, and sequential current fluctuations of different magnitude are observed. The drift to lower magnitudes of current is due to an increase in the IR drop across the cell during the experiments, as expected due to the ohmic effects associated with the screening of the electrode surface by attached bubbles [23]. In the traces of Fig. 2, current drifts followed by sharp returns to the baseline indicate the occlusion of the electrode surface by bubbles attached to it. As the bubbles grow, they cover an increasingly large portion of the cathode surface, which translates into a decrease in magnitude of the current. Large bubbles are formed by a coalescence process where smaller bubbles progressively join together to form bigger ones. When a bubble detaches, the entire surface formerly occluded is suddenly available for hydrogen reduction, which leads to the sharp increase in current. Hence, the size of the released bubbles can be estimated from the sharp steps in the time sequence. The low amplitude oscillations are related to an evolving stream of small bubbles, whereas bigger oscillations correspond to the release of a larger bubble. The steps in the figure indicate that bubbles of different sizes form on the 5.4 mm electrode, but the largest bubbles occlude about 5 % of the cathode surface, corresponding to a circle of radius of 0.6 mm.

The maximum bubble size in this configuration is reduced by the magnetic field. Since the electrode is vertical, with a vertical field parallel to the electrode surface, the flow generated by the Lorentz force across the surface (as shown the inset in figure 1a) tends to dislodge the hydrogen bubbles as they form. The enhancement of the hydrogen current of up to 25 % in large fields is due, at least in part, to less of the cathode area being occluded by bubbles.

We also observed that the stream consisted of small bubbles spread throughout the electrolyte due to convection. At high fields (>3 T) the transparency of the solution was changed by the presence of many very small bubbles. The time needed for the cloudiness to

disappear completely was 2-5 minutes. Matsushima et al [13] had previously described the solution becoming cloudy when hydrogen was evolving under an applied field.

3.1.2 *Noise spectra:* In order to examine the bubble formation more closely, we used a microelectrode to measure the electrochemical noise spectra. With such small electrode we amplify the screening effect of a single bubble on the measured signal. The effect of different current densities and field intensities on the hydrogen production were investigated. The 130 μm vertical microelectrode was immersed in the horizontal field of the electromagnet, so that the resulting Lorentz force acted upwards or downwards. The electrolyte was again 1.2 M H_2SO_4. Single bubbles were released from the electrode surface at a regular rate. Figure 3 (a) shows the noise spectra for fixed B = 1.5 T when *j* varied from 1 to 20 A cm^{-2}, with the *Lorentz force acting downwards*. The main peak at low frequency corresponds to the periodicity of the bubble release. The more regular the release, the more harmonics are observed. It is seen that increasing current decreases the frequency of the main peak from 6 Hz to 4 Hz, while at constant current density of 3.5 A cm^{-2} the frequency decreases from 17 Hz in zero field to 5.7 Hz in 1.5 T, as shown in Fig. 3(b). The high frequency segment of the noise spectra varies as $1/f^{\alpha}$, where $\alpha \approx 2$. Figure 3 (c) is a plot which summarizes the results in (a) and (b), showing the decrease of frequency of bubble release at constant current, j = 3.5 A cm^{-2}, as well as the effect of changing the current at fixed field. Note that the data do *not* show a positive slope, nor do they scale with *jB*, as would be expected.

To investigate whether there was any effect of Lorentz force direction on the frequency of hydrogen bubble detachment, noise spectra were compared when the Lorentz force acted upwards or downwards on bubbles grown at the microelectrode at a high current density. As seen in Fig. 4, for a given magnitude of the magnetic field (1.5 T), when F_L *acts downwards* there is a clear characteristic peak around 4 Hz, together with the harmonics, whereas when F_L *acts upwards* no characteristic peak is seen. There we observed a column of very small bubbles emerging from the electrode at high frequency without any evident periodicity, whereas, when F_L acts downwards bigger bubbles are observed leaving the electrode at slower rate. The periodic release observed by eye is related to the overpotential oscillations. Figure 4(b) shows these oscillations for j = 20 A cm^{-2}, at 0 T and in an applied field of 1.5 T or -1.5 T. The electrode was photographed with

a video camera and the bubble radius with F_L acting downwards was 247 ± 35 μm just before detachment. The release frequency is f = 4.3 ± 0.1 Hz. The bubble size exceeds that of the microelectrode by a factor 4. Calculation of bubble volume is addressed in the discussion section.

As can be seen from this example, the overpotential signal gives characteristic information of the process for a single-bubble regime. We clearly observed that there is a relation between the oscillation frequency and bubble size, and that the process can be periodic.

The periodic release of bubbles at the microelectrode leads to a characteristic shape of the noise spectrum. The power spectral density, PSD, is constant until the main peak appears; this is followed by its harmonics while PSD decreases inversely with f. Then a second plateau appears before the tail is formed towards high frequencies. When PSD varies, it follows a $1/f^2$ relation before reaching the noise floor, at above about 10 kHz.

When the system was subject to high rate of hydrogen production in a convective regime promoting the vertical upwards movement, the second plateau is extended, as shown in Fig.4. Similar high-frequency behaviour has been reported for hydrogen evolution from solution by Szenes et al [22].

The measurements taken at fixed current density were accompanied by a reduction in the measured overpotential of around 100 mV in the 1.5 T field. The same phenomenon was observed for water electrolysis from a Na_2SO_4 aqueous solution, as reported by Diao and coworkers [21]. Similarly to the results obtained for a fixed overpotential with changing field, the increased value of the measured signal in this case is related to the screening effect of the bubbles on the electrode surface [23].

We see that the magnitude and direction of the Lorentz force strongly affects the bubbling regime. In a regime where multiple bubbles are produced (the case of a big electrode) increasing Lorentz force acting sideways reduces the bubble size. In a regime where single bubbles are released in a sequence, the Lorentz force acting in the same direction than buoyancy reduces the bubble size producing a stream of small bubbles with no periodicity. On the contrary, if F_L acts opposite to buoyancy, it stabilizes the growing bubbles and those grown more rapidly, at high current density tend to be bigger.

3.2 *The copper/hydrogen system.*

3.2.1 *Electrochemical characterization:* The field effect on hydrogen release from the copper substrate was also investigated while the interface grows, as protons and cupric ions are co-reduced. The cyclic voltammograms of Fig. 1(b) show the cathodic η-*j* relationship for copper in contact with a 0.3 M $CuSO_4$ + 1.2 M H_2SO_4 solution, taken from the open circuit potential to η = -1.5 V, and the corresponding effect of magnetic fields up to 5 T. It is seen that the copper reduction reaction is mass transport controlled in an overpotential window ranging approximately from -0.4 V to -0.8 V at 0 T where a current density plateau (j_L) marks the limit between two regimes. Below the limiting value of the ratio $j/j_L < 1$, growth is not expected to exhibit structures associated with mass transport control. Above it, where $j/j_L > 1$, mass transport is relevant and determines growth structures. Moreover, at such high currents hydrogen reduction is occurring as a side reaction.

In a system where mass transport controls the ongoing reaction, depletion of the ion concentration with time is expected under galvanostatic control. As seen from Fig. 1 (b), field imposition increases the value of limited current density j_L due to magnetoconvection thus extending the region for which $j/j_L < 1$. The field also increases the measured current values in the region for which $j/j_L > 1$. Based on these identified regions we performed a series of experiments aimed to characterize quantitatively and morphologically the field effect on the copper-hydrogen co-reduction system.

Figure 5 shows chronoamperometry of the first 10 seconds of galvanostatic deposition performed at $j = 0.07$ A cm^{-2}, with and without field. It is observed that in zero field the overpotential increases sharply. This is due to the fact that, at this particular current density, the system presents a double value of the potential (Fig 1 (b)). When the system starts reducing copper, the corresponding voltage is around η = -0.2 V. Then, under predominant mass transport limited conditions and with depletion of copper ions, the overpotential increases to approximately -0.75 V to keep up with the imposed current density. In this case reduction of protons and cupric ions proceeds simultaneously. When a field is applied, however, mass transport conditions are enhanced due to the stirring effect of the Lorentz force, Eq. 1. The potential is no longer double-valued, and the conditions

allow the system to maintain the imposed current at a lower corresponding overpotential of about -0.3 V. These results are in good agreement with the responses observed by Nikolić [24] who reported reductions in the effective overpotential when a strong hydrodynamic regime was established in copper-hydrogen co-reduction from acid sulphate solutions.

3.2.2 *Morphology:* The effect of bubbles of hydrogen evolved during copper growth was mainly characterized by scanning electron microscopy. Deposits were grown on 5 mm vertical Cu sputtered electrodes immersed in vertical fields from a 0.3 M $CuSO_4$ + 1.2 M H_2SO_4 solution; in this case the *Lorentz force acts sideways*. The growing surface around bubbles allows an indirect estimation of bubble size from the appearance of pores. Observations of the imprints of hydrogen co-reduced bubbles were first reported by Devos et al during nickel deposition [8]. In the hydrogen evolution regime, we find that copper sometimes grows around bubble's walls and projects itself into the solution, as seen in figure 6(a) where a copper stockade surrounding a bubble site is shown. In this case the deposit was grown for 25 s at η = - 1.0 V at 0 T. Fig. 6 (b) shows, for the same conditions, the cross section view of copper growth at the walls of the pores caused by two adjacent hydrogen bubbles. It is seen that the site which was occluded by the bubbles exhibits a flat surface, indicating that no copper ions had access to that portion of the electrode. Figure 6 (c) shows a dendrite of the same sample, illustrating the irregularity of the deposit.

Figures 6 (d) and (e) show the case when a 4 T field is applied. In (d) a site is shown where small bubbles of sizes ranging between 50 nm and 1 μm in diameter were produced. Elongated features correspond to copper growth around two or three bubbles aroused in a row. Fig. 6 (e) is a wider view of the same zone, showing a gradient of deposit thickness where a big bubble grew. It is likely that it formed by coalescence of smaller bubbles, as suggested by (d). The image in 6 (d) shows pores in a very small size range, well below minimum sizes around 150 μm observed by Matsushima and coworkers during production of single H_2 bubbles at Pt electrodes from KOH solution [25]. Our minimum pore sizes agree with reports by Kikuchi and coworkers who studied hydrogen formation on Pt electrodes from solutions containing sulphuric acid [26], albeit at low current densities. Matsushima uses a lower value(~0.25 A cm^{-2}), but the critical radius for a stable nucleus is reported strongly dependent on current density by Vogt [27]

When a magnetic field is applied during copper electrodeposition performed galvanostatically at current density values corresponding to HER, the features observed in the deposit change. Figure 6 (f) and (g) show SEM images of copper deposits obtained at 0 T and 4 T, respectively, after just 5 s of growth under galvanostatic conditions with a current density of j = 0.07 A cm^{-2}. The effect of a 4 T field on the morphology is drastic. In 0 T, the growth is dendritic, accompanied by hydrogen evolution. When the field is applied, the morphology changes dramatically: the copper deposit does not project any tips into the solution but the growth is planar. Facetted growth features appear as parallel successive steps in the deposit. The image clearly indicates the expected change in growth mode to a regime where mass transport does not control morphology. This agrees with the overpotential values in Fig. 5, around η = -0.75 V at 0 T, in contrast with η = -0.28 V under 4 T, where hydrogen is not produced. The former value is located around the onset of hydrogen evolution according to the cyclic voltammogram in Fig. 1(b). Roughness measurements taken by atomic force microscopy of the surface shown in Fig. 6 (g) indicate a rms value of just 19 nm, which is very smooth, in contrast to typical values one order of magnitude higher for the sample shown in (f).

3.2.3 *Current efficiency:* In order to quantify the field effect on the hydrogen evolution during copper electrodeposition, the electrochemical quartz crystal microbalance (EQCM) was used to separate the fraction of the current belonging to copper from that corresponding to hydrogen. The electrode was again oriented vertically in the electromagnet. Potentiostatic and galvanostatic measurements were performed, growing a layer of copper on top of a gold-plated quartz crystal from the 0.3 M $CuSO_4$ + 1.2 M H_2SO_4 solution.

The current and microbalance frequency were recorded as a function of time, and the impedance matching method was used to calculate the change in mass [28]. The copper current was extracted from the change in mass via:

$$I_{Cu} = \frac{\mathrm{d}m}{\mathrm{d}t}\frac{nF}{m_{Cu}} \qquad (2)$$

where $\mathrm{d}m/\mathrm{d}t$ is the time derivative of the measured mass, n = 2 is the number of electrons transferred, F is Faraday's constant and m_{Cu} is the molar mass of the depositing ion.

Figure 7 shows examples of the effect of a 1.5 T field for the case of potentiostatic deposition at η = -1.0 V. In (a) and (b) the curves obtained for B = 0 T and B = 1.5 T are shown respectively. It can be seen from the data that the current efficiency of nearly 90 % obtained after 15 seconds at 0 T is reduced to approximately 75 % by the applied field, indicating that the field enhances the hydrogen current more than the copper current in these conditions.

The EQCM measurements were also performed galvanostatically with a current density j = 0.15 A cm^{-2} (which corresponds to η = -1.0 V at 0 T), chosen in order to ensure intense hydrogen reduction. It was found that the efficiency increases from about 4% in 0 T to 40% in 1.5 T. This was accompanied by a drop in overpotential of approximately 0.5 V, which agrees with data in Figs. 1(b), 5 and 6 (f, g).

EQCM measurements confirm quantitatively the inference from voltammetric plots, that fields increase current efficiency during Cu-H co-reduction when the system is under galvanostatic control, provided that the imposed current density is around the diffusion limited value, j_L. The importance of this relies on the fact that mass transport-enhanced conditions promoted by magnetoconvection allow the system to operate at significantly lower overpotentials, which in turn leads to smother deposits and diminishes or inhibits hydrogen reduction. Popov et al recently reported, for the acid copper system, that convection induced by pulsed deposition can similarly improve surface roughness and improve current efficiency with view to energy saving [29]. The EQCM measurements also show that the magnetic field increases hydrogen current when the system is under potentiostatic control, reducing plating efficiency in that case.

3.2.4 *Noise spectra:* Here, we illustrate two cases using as a parameter the ratio between the applied current density j and the mass transport-controlled copper current density j_L. One is when $j/j_L \approx 1$ and the other is when $j/j_L >> 1$. In the former case, field imposition promotes a change in growth mode while in the latter it does not. A vertical sputtered copper electrode of 5 mm diameter was used, immersed in a horizontal field.

The power spectral density is plotted as a function of frequency in Fig 8(a) for the 5 mm electrode at a current density of j = 0.07 A cm^{-2}, $j/j_L \approx 1$, and a change in growth mode is observed as a result of magnetically induced convection (figures 5, 6f and 6g). The two

orders of magnitude reduction of low frequency noise under the 1.5 T field (Fig 8a) reflects the suppresion of hydrogen evolution on the working electrode surface, due to the lower overpotential obtained in the galvanostatic mode. It is expected that the noise spectra show the effect of surface area modification due to copper growth. In this regard, we note that in all cases with copper-containing solution the noise follows a $1/f^{\alpha}$ relation around 1 Hz with α larger than 2. We relate this to the non-stationarity of the system, as copper deposition is continously modifying the effective area of the working electrode thus introducing changes in the noise spectra, as compared with similar conditions in a copper-free solution. The noise spectrum in Fig 8(a) at 1.5 T corresponds to planar growth in an overpotential of about 0.3 V, with no hydrogen bubbling (Fig 6g). There is no plateau and no peaks in this growth mode, where $j/j_L < 1$. The noise spectrum in zero field corresponding to the case when $j/j_L \approx 1$ shows an incipient plateau at the lowest frequency, and much greater noise due to hydrogen bubble release.

The case when $j/j_L >> 1$ is illustrated in Fig 8 (b) for the 130 μm diameter microelectrode. The effect of Lorentz force direction was also examined for this system. The low frequency plot in zero field shows a low broad peak around 12 Hz, indicating that hydrogen bubbles are released at roughly this characteristic frequency. When 1.5 T is applied, the signal is flattened, and there is no longer any characteristic frequency for bubble release. Although this is valid whether when F_L acts up or down, the effect is more pronounced when it acts in the same sense as the buoyancy force. This is similar to what was found for the copper-free system (Fig 4).

In this case where vigorous hydrogen formation accompanies rapid copper surface growth, the noise spectra show a longer plateau at low frequencies, resembling the shape associated with hydrogen bubbling. The extent of the plateau is narrower than that observed for the copper-free system.

4. Discussion.

We begin by discussing some aspects of the hydrogen evolution in the copper-free electrolyte. A striking feature of the microelectrode data is the regular, periodic nature of the bubble release (Figs 3, 4). The bubbles grow to a certain size, and then detach from the electrode. The size increases substantially in a magnetic field, and with increasing current

density. For instance, the bubble volume is over 20 times greater for j = 20 A cm^{-2} and B = 1.5 T than it is for j = 3.5 A cm^{-2} and B = 0. To gain some insight into the phenomenon, we consider the data in Fig 3 where the microelectrode surface is vertical, and the applied field is horizontal. In this configuration, the bubbles simply grow to a certain radius r, and are then swept away. Bubble release is periodic, with frequency f. In the absence of field, f = 17 Hz, so each bubble grows for 59 ms. The pressure of hydrogen inside the bubble is close to atmospheric pressure P_0. Corrections are $h\rho g$ due to the depth h of the electrolyte of density ρ above the microelectrode surface, and the pressure difference $2\gamma/r$ across the curved surface of the bubble, where $\gamma \approx 70$ mN m^{-1} is the surface tension of water. Both these corrections amount to less than 1% of P_0 and can safely be neglected. The size of the bubble that grows in a time $1/f$ under galvanostatic conditions with a current density j is deduced from the gas law

$$P_0 V = \mathrm{n}RT \tag{3}$$

and Faraday's law for H_2

$$n = \pi r_e^2 j/2\mathrm{F}f \tag{4}$$

where F is 96485 C mol^{-1}. Hence the radius of the bubble, assumed to be spherical, is

$$r = (3r_e^2 j\mathrm{R}T/8\mathrm{F}fP_o)^{1/3} \tag{5}$$

Taking f = 17 Hz and r_e = 65 μm gives r = 94 μm, which is actually a bit bigger than the electrode, but consistent with visual observations. In the example of Fig 4(b), where f = 4.3 Hz, the calculated bubble radius is 257 ± 2 μm, in good agreement with the radius obtained by direct observation of 247 ± 35 μm. The angle θ (see Fig. 3c) when the bubble detaches is given by $\sin\theta = r_e/r$. In the present case θ = 44°, and the horizontal force $2\pi r_e\gamma\sin\theta$ holding it to the electrode is 20 μN. It should be noted that this is much greater than the upthrust given by Archimedes principle, $V\rho g$ = 0.03 μN. The radius of the bubble when the upthrust balances the surface tension is about 300 μm [27]. Convective forces must be at play to sweep off the bubble, even in the absence of a magnetic field. There will be very large current densities around the edge of a microelectrode bearing a large bubble, which may lead to turbulence there.

The bubble growing on the microelectrode is more stable in a magnetic field when the Lorentz force acts downwards (Fig 4). The effect of the applied magnetic field at constant current in Fig 3(c) is to reduce *f*, so the bubbles grow to three times the volume before they detach. When the current increases from 1 A cm^{-2} to 20 A cm^{-2} at constant field, the frequency of release would be expected to increase from 6 Hz to 16 Hz if the bubbles were the same size when they are released. In fact they grow much bigger, and the release frequency is reduced to 4 Hz. At first sight this is surprising; the field was expected to create a transverse flow which tends to dislodge the bubble, especially at high current density. The opposite is observed; the bubble radius in the applied field approaches that expected for release governed by upthrust [27]. Data (not shown here) in a vertical field with a horizontal microelectrode surface confirm the trend (a reduction in bubble release frequency from 5 Hz in zero field to 0.5 Hz in 5T). This suggests that the convective movement of charged ions might be somehow damped by the applied field. The damping force is

$$F_d = \sigma v \times \boldsymbol{B} \times \boldsymbol{B} \qquad (6)$$

where σ is the conductivity of the electrolyte. In the present case $\sigma \approx 100$ S m^{-1}. However, assuming $v \approx 0.1$ m s^{-1} and taking $j = 3.5\ 10^4$ A m^{-2}, the damping force only exceeds the Lorentz force when $B > 1000$ T. We speculate that high-frequency modes of oscillation play a critical role in bubble release, and that the field damping is much more effective than our estimate suggests.

An important lesson from the data in Fig 3(c) is that the hydrogen bubble release is *not* primarily governed by the Lorentz force. The data do not scale with *jB*, and the lines have the opposite slope to that expected. The current density has relatively little influence on the release frequency, whereas it is greatly influenced by the magnetic field. It is possible that turbulence created by current crowding around the rim of the microelectrode could be suppressed by a magnetic field.

A feature of the electrochemical noise spectra is the corner frequency, above which there is a decrease of the noise power with $1/f^{\alpha}$ slope, with α near 2. This slope can be attributed to a growth-coalescence process as described in [21]. Although the main peak

and its harmonics are suppressed when the Lorentz force acts in the same sense as buoyancy force, the general shape of the spectrum is not modified.

The electrochemical noise measurements in the co-reduction regimes where the ratio j/j_L was below, near and above 1 allowed us to observe the characteristic spectra in the presence of surface modification due to growth. When copper deposition and hydrogen evolution both occur at the electrode surface, the periodic release of the hydrogen bubbles is strongly modified. Under zero field, a weak peak near 12 Hz is still visible for the microelectrode, but there are no harmonics (bubble evolution is not very regular). When the 1.5 T field is applied, the peak disappears. Compared to the case where only hydrogen evolution occurs, the corner frequency above which the noise power follows a $1/f^2$ law is shifted to lower frequency, from a few hundred Hz to about 10 Hz. The shift in corner frequency and the disappearance of periodicity in the bubble release may be related to the constantly-changing, rough nature of the copper cathode. The slope with $\alpha > 2$ indicates that the electrode is not stable, but is evolving.

As regard current efficiency, for the configuration where the Lorentz force helps to sweep off hydrogen bubbles from a vertical electrode (figures 5, 6 and 7), our results indicate that during potentiostatic copper electrodeposition at high overpotential, enhanced hydrogen evolution in the field decreases the current efficiency to around 75%. The morphology of deposits obtained in this configuration indicates that the deposit morphology under field is improved, whether the deposition is potentiostatic or galvanostatic. In the former case it becomes smoother and the pore size is greatly diminished, although less copper is produced due to a reduction in plating efficiency. The efficiency reduction and the deposit smoothness may be linked, in that the bubble size is diminished for this configuration.

Shinohara et al [30] explain the inhibition of dendritic growth of a copper deposit by a micro-MHD effect. The interaction of the field with the current lines converging on specific surface features produces a short-range convective effect, creating a microvortex in the vicinity of a protrusion. The micro-MHD effect may influence the morphology obtained under potentiostatic control. Tip growth at the solid-liquid interface depends on the local current distribution. When it is non-uniform, tips face a higher concentration gradient

compared to the zones nearby, and therefore grow faster, depleting ions from the surrounding area. Any homogenization of the current distribution leads to a more uniform growth rate, hence promoting smoother deposits. Homogenization by convection is only possible when the tips are bigger in size than the diffusion layer. Our observations of reductions in pore size on scales well below 1 micron, lead us to suggest that a micro-convective regime is promoted by the magnetic field. The interaction of magnetic field with current distribution on the micron scale would provide the conditions necessary for a more uniform distribution of ions in the electrolyte close to the electrode surface, thus leading to an enhancement in deposit quality. The microconvection at the surface can promote the release of small hydrogen bubbles.

When the co-reduction of hydrogen and copper was performed galvanostatically, the morphology is improved due to overpotential reduction by the magnetic field. In this case, the system is forced to maintain a fixed rate of reaction. When the diffusion layer thickness is reduced by magnetoconvection, the system has a degree of freedom and the way to lower the reaction rate is to reduce the driving force. This means a reduction in overpotential, with a corresponding reduction in hydrogen reduction current and a change in copper growth mode, since the equilibrium has been moved to a regime where the deposits grow uniformly. Similar effects of convection are found for copper deposition from acid solutions [24, 29].

5. Conclusions

The formation of hydrogen bubbles and their frequency of release from copper electrodes are strongly influenced by an applied magnetic field, particularly by the resulting magnetoconvective direction. Although the hydrogen evolution is influenced by the interplay of the Lorentz and buoyancy forces, the Lorentz force does seem to be the principal consideration governing bubble release. The magnetic field has the effect of stabilizing a growing bubble on a microelectrode when the Lorentz force opposes buoyancy, especially at high current densities. When Lorentz and buoyancy sum up, the bubbles are swept off the electrode earlier than at zero field. The physical reason for this

has not been determined, but further experiments with horizontal electrodes of different sizes are needed to explore what seems to be a new effect in magnetoelectrochemistry.

We have illustrated the specific features of the electrochemical noise spectrum for the cases of periodic and non-periodic release of hydrogen gas from a copper microelectrode. The slope in the kilohertz range revealed a characteristic $1/f^2$ dependence corresponding to coalescence of microbubbles.

When copper is being deposited, three regimes are distinguished: planar growth when $j < j_L$, mass transport-limited growth with incipient hydrogen reduction when $j \approx j_L$ and mass transport-limited with strong bubbling when $j > j_L$. A distinctive noise spectrum is found in each regime.

Hydrogen co-reduction with copper is enhanced in a magnetic field when the cell is under potentiostatic control, but it is possible to reduce or even suppress it entirely at fixed current under galvanostatic control. The morphology of the deposits is improved by the field in either case. At high overpotentials the field enhances both copper and hydrogen currents but it has the greater effect on the hydrogen, reducing copper plating efficiency. In this case the films are smoother, due probably to the micro-MHD effect.

Application of a magnetic field during galvanostatic growth of copper films inhibits or suppresses hydrogen evolution by drastically reducing the effective overpotential when the system is set to a regime where $j/j_L \approx 1$. Controlling the system galvanostatically in a magnetic field is an efficient way to produce smooth films at cell potentials lower than is possible without a convective system. This implies an energy saving in the plating process.

Acknowledgements

This work was supported by Science Foundation Ireland, as part of the MANSE project 05/IN/1850. We are grateful to Dr. Colm Faulkner for help with the FIB sectioning.

References

[1]. H.C. Shin, J. Dong, M. Liu, Adv. Mater. 15 (2003) 1610.

[2]. S. Li, R. Furberg, M.S. Toprak, B. Palm, M. Muhammed, Adv. Funct. Mater. 18 (2008) 2215.

[3]. H.C. Shin, M. Liu, Adv. Funct. Mater. 15 (2005) 582.

[4]. W. Huang, M. Wang, J. Zheng, Z. Li, J. Phys. Chem. C 113 (2009) 1800.

[5]. T. Z. Fahidy J. Appl. Electrochem 13(1983) 553.

[6]. T.Z. Fahidy, Prog. Surf. Sci. 68 (2001) 155.

[7]. G. Hinds, F.E. Spada, J.M.D. Coey, T.R. Ní Mhíocháin, M.E.G. Lyons, J. Phys. Chem B 105 (2001) 9487.

[8]. O. Devos, A. Olivier, J.P. Chopart, O. Aaboubi, G. Maurin, J. Electrochem. Soc. 145 (1998) 401.

[9]. A. Bund, A. Ispas, J. Electroanal. Chem. 575 (2005) 221.

[10]. M. Uhlemann, A. Krause, A. Gebert, J. Electroanal. Chem. 577 (2005) 19.

[11]. A. Krause, M. Uhlemann, A. Gebert, L. Schultz, E. Acta 49 (2004) 4127.

[12]. J.A. Koza, M. Uhlemann, A. Gebert, L. Schultz, E. Acta 53 (2008) 5344.

[13]. H. Matsushima, D. Kiuchi, Y. Fukunaka, E. Acta 54 (2009) 5858.

[14]. J.A. Koza, M. Uhlemann, A. Gebert, L. Schultz, Electrochem. Commun. 10 (2008) 1330.

[15]. J.A. Koza, S. Mühlenhoff, M. Uhlemann, K. Eckert, A. Gebert, L. Schultz, Electrochem. Commun. 11 (2009) 425.

[16]. C. Gabrielli, F. Huet, M. Kedam, J. Electrochem. Soc. 138 (1991) L82.

[17]. A. Benzaïd, F. Huet, M. Jèrôme, F. Wenger, C. Gabrielli, J. Galland, E. Acta 47 (2002) 4315.

[18]. U. Bertocci, C. Gabrielli, F. Huet, M. Keddam, P. Rosseau, J. Electrochem. Soc. 144 (1997) 37.

[19]. C. Gabrielli, F. Huet, M. Keddam, A. Sahar, J. Appl. Electrochem. 19 (1989) 683.

[20]. A. Steyer, P. Guenoun, D. Beysens, Phys. Rev. Lett. 68 (1992) 1869.

[21]. Z. Diao, P.A. Dunne, G. Zangari, J.M.D. Coey, Electrochem. Commun. 11 (2008) 740.

[22]. I. Szenes, G. Meszaros, B. Lengyel, E. Acta 52 (2007) 4752.

[23]. C. Gabrielli, F. Huet, R. P. Nogueira, E. Acta 50 (2005) 3726.

[24]. N.D. Nikolić, K.I. Popov, Lj.J. Pavlović, M.G. Pavlović, J. Electroanal. Chem. 588 (2006) 88.

[25]. H. Matsushima, D. Kiuchi, Y. Fukunaka, K. Kuribayashi, Electrochem. Comm. 11 (2009) 1721.

[26]. K. Kikuchi, H. Takeda, B. Rabolt, T. Okaya, Z. Ogumi, Y. Saihara, H. Noguchi, J. Electroanal. Chem 506 (2001) 22.

[27]. H. Vogt, Ö. Aras, R. J. Balzer, Int. J. Heat Mass Transfer 47 (2004) 787.

[28]. C.S. Lu, O. Lewis, J. Appl. Phys. 43 (1972) 4385.

[29]. K.I. Popov, N.D. Nikolić, P.M. Zivković, G. Branković, E. Acta 55 (2010) 1919.

[30]. K. Shinohara, K. Hashimoto, R. Aogaki, Electrochemistry 70 (2002) 773.

Figure 1. Cyclic voltammetry at 0.2 V s^{-1} showing the effect of vertical magnetic fields up to 5 T when a Cu electrode of 5.4 mm in diameter is vertically immersed in (a) a 1.2 M H_2SO_4 electrolyte and (b) a 0.3 M $CuSO_4$ + 1.2M H_2SO_4 electrolyte. The insets in (a) show the electrode configuration and the field dependence of the current.

Figure 2. Time sequences (chronoamperometry) measured at η = -1.0 V for the 5.4 mm electrode in the conditions of Fig. 1 (a).

Figure 3. Electrochemical noise spectra showing the effect of current density and field intensity on hydrogen evolution from a 130 μm diameter vertical Cu microelectrode in a horizontal magnetic field. The electrolyte is 1.2 M H_2SO_4. (a) Constant B = 1.5 T and j varying between 1 and 20 A cm^{-2}. (b) Constant j = 3.5 A cm^{-2} and varying B between 0 and 1.5 T. (c) Frequency of bubble release as a function of the jB product.

Figure 4. (a) Electrochemical noise spectra of the Cu microelectrode in a vertical orientation for a current density j = 20 A cm^{-2}, measured for a 1.5 T horizontally applied magnetic field oriented in two opposite senses. (b) Corresponding overpotential oscillations obtained for the same conditions and at 0 T.

Figure 5. Chronoamperometry of the first 10 seconds of galvanostatic deposition performed at j = 0.07 A cm^{-2}, with and without field for a 5.4 mm Cu electrode vertically immersed in a 0.3 M $CuSO_4$ + 1.2 M H_2SO_4 electrolyte.

Figure 6. Electron micrographs showing features observed in Cu deposits grown from a 0.3 M $CuSO_4$ + 1.2 M H_2SO_4 electrolyte. For potentiostatic deposition at η = -1.0 V for 25 s in zero field (a) a feature surrounding the location of a hydrogen bubble, (b) a side view of two coalesced pores and (c) an enhanced dendrite. For potentiostatic deposition at η = -1.0 V for 25 s in 4 T: (d) pores and (e) thickness gradient surrounding small bubbles that coalesced into a bigger one during deposition. For galvanostatic control during 5 s at j = 0.07 A cm^{-2}, the morphology obtained under (f) 0 T and (g) 4 T.

Figure 7. Magnetic field effect on copper and hydrogen partial reactions, as derived from electrochemical quartz crystal microbalance measurements. The electrolyte is 0.3 M CuSO4 + 1.2 M H_2SO_4. Copper current is obtained from the frequency measurements and

the current difference is assumed to be due to hydrogen reduction. (a) Potentiostatic reduction at η = -1 V, 0 T; (b) potentiostatic reduction at η = -1 V, 1.5 T.

Figure 8. Electrochemical noise spectra of the working electrode potential during copper deposition under zero field and 1.5 T under galvanostatic control. (a) When hydrogen evolution is suppressed, j = 0.07 A cm^{-2}. (b) When strong hydrogen co-reduction is produced at j = 20 A cm^{-2}. We compare in the graph the effect of F_L orientation. The electrolyte is 0.3 M $CuSO_4$ + 1.2 M H_2SO_4. The black line shows $1/f^2$ slope. Data shown are undersampled to 1000 Hz from the 100 kHz raw data.

Figure(s)

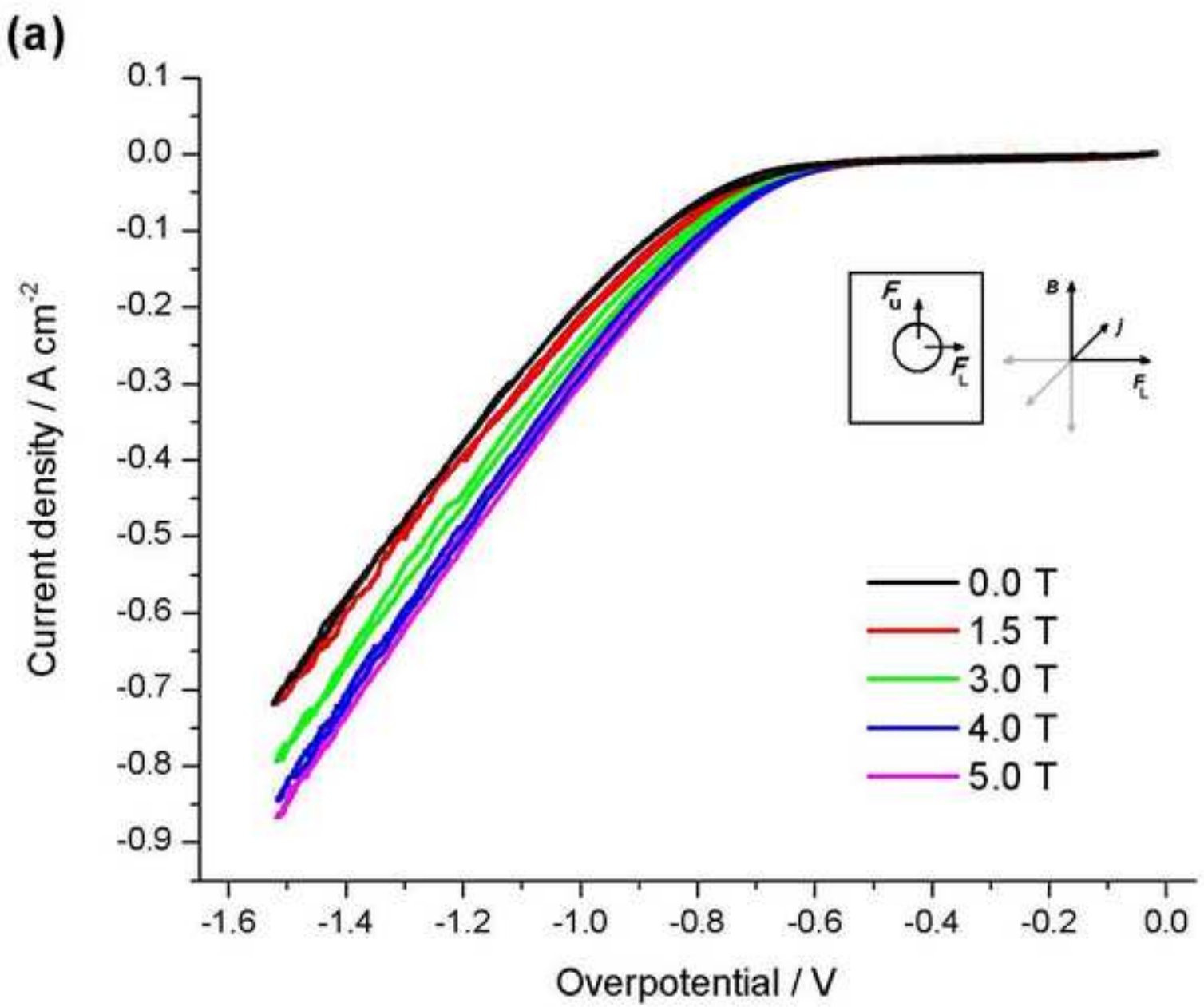
(a)
Current density / A cm-2
0.1
0.0
-0.1
-0.2
-0.3
-0.4
-0.5
-0.6
-0.7
-0.8
-0.9
-1.6
-1.4
-1.2
-1.0
-0.8
-0.6
-0.4
-0.2
0.0
Overpotential / V
0.0 T
1.5 T
3.0 T
4.0 T
5.0 T
B
J

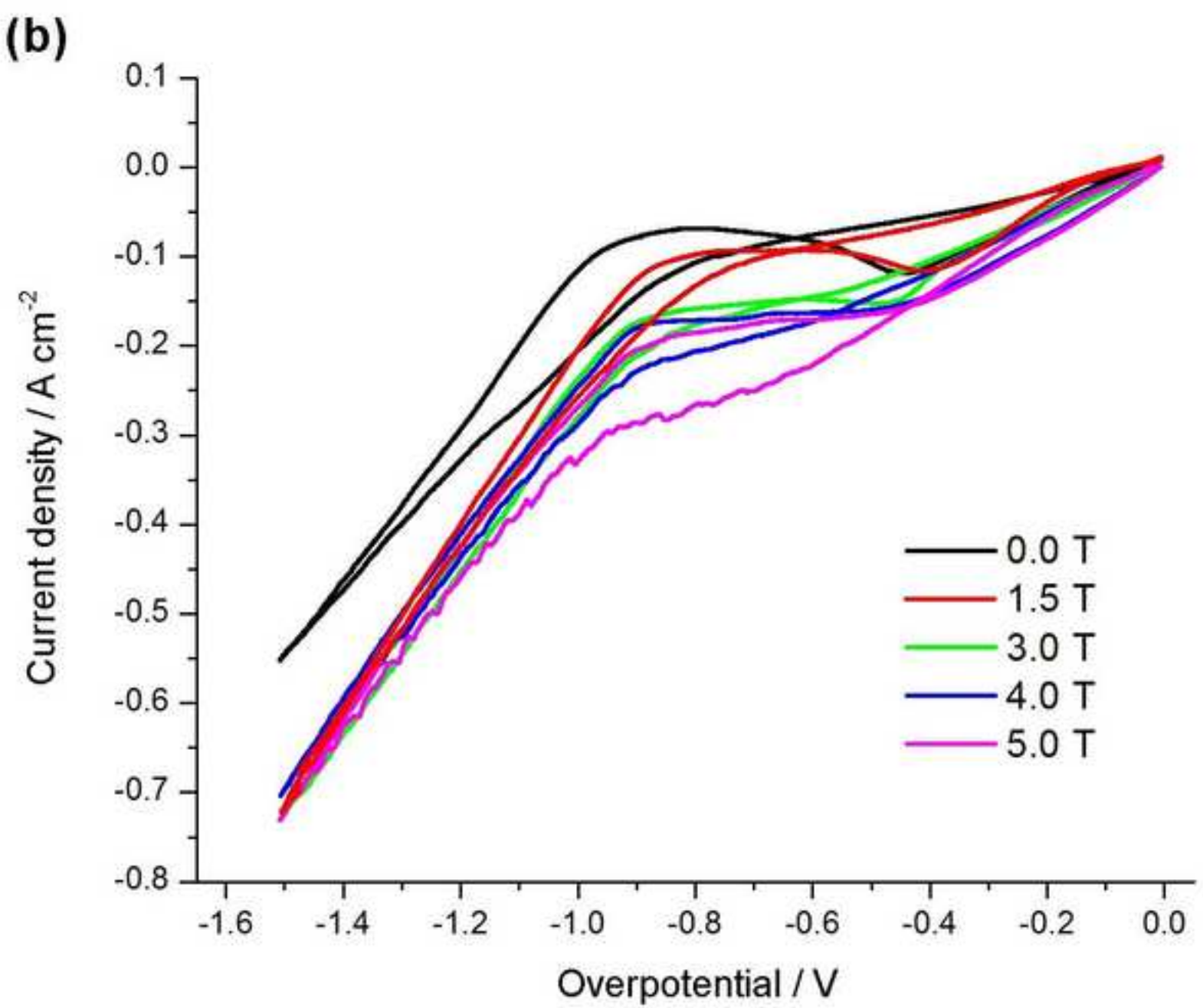
(b)
Current density / A cm-2
Overpotential / V
0.1
0.0
-0.1
-0.2
-0.3
-0.4
-0.5
-0.6
-0.7
-0.8
-1.6
-1.4
-1.2
-1.0
-0.8
-0.6
-0.4
-0.2
0.0
0.0 T
1.5 T
3.0 T
4.0 T
5.0 T

Figure(s)

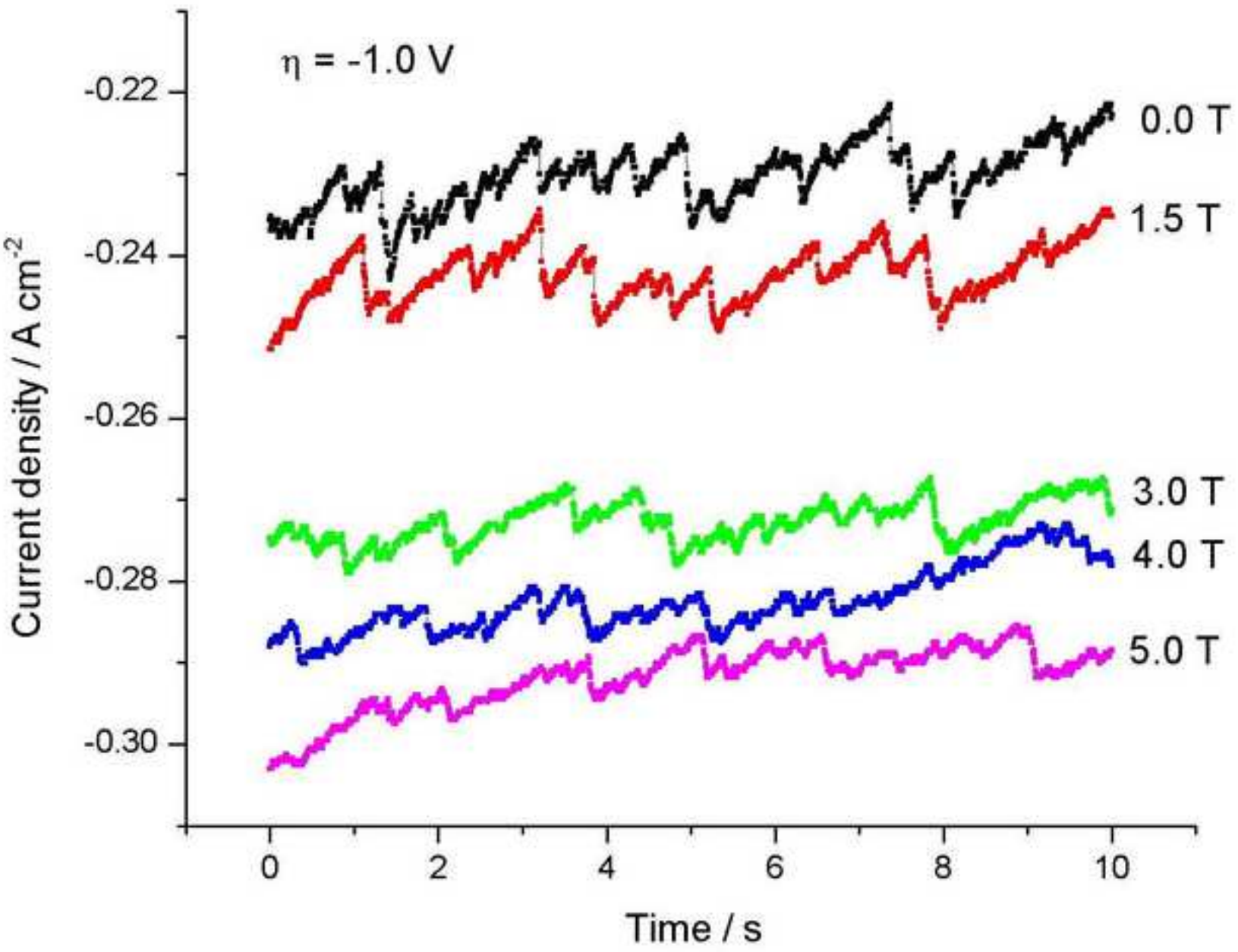
η = -1.0 V
-0.22
-0.24
-0.26
-0.28
-0.30
Current density / A cm-2
0.0 T
1.5 T
3.0 T
4.0 T
5.0 T
0
2
4
6
8
10
Time / s

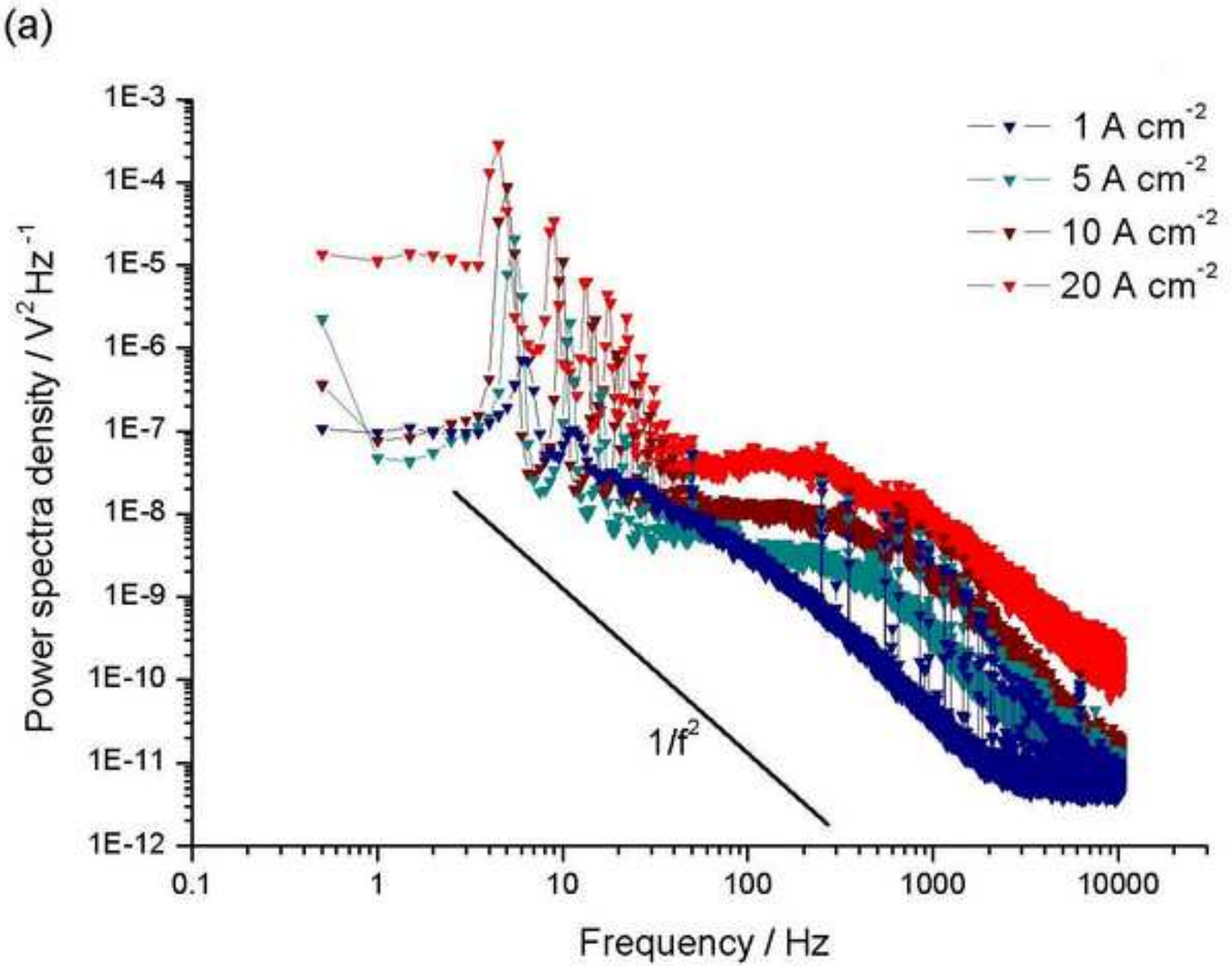
(a)
Power spectra density / V^{2}Hz^{-1}
1E-3
1E-4
1E-5
1E-6
1E-7
1E-8
1E-9
1E-10
1E-11
1E-12
0.1
1
10
100
1000
10000
Frequency / Hz
1/f^2
1 A cm^{-2}
5 A cm^{-2}
10 A cm^{-2}
20 A cm^{-2}

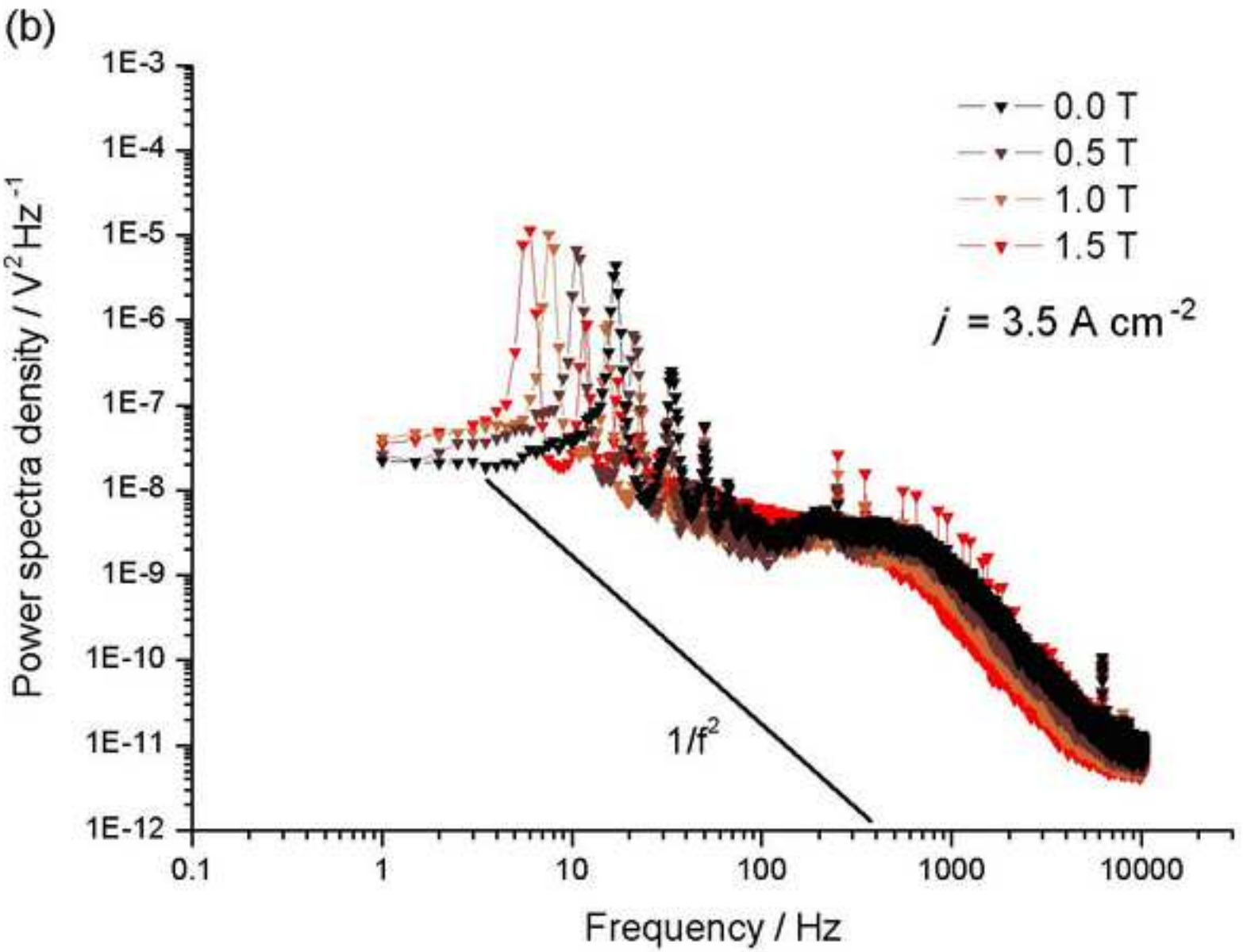
(b)
Power spectra density / V^2 Hz^{-1}
1E-3
1E-4
1E-5
1E-6
1E-7
1E-8
1E-9
1E-10
1E-11
1E-12
0.1
1
10
100
1000
10000
Frequency / Hz
0.0 T
0.5 T
1.0 T
1.5 T
j = 3.5 A cm^{-2}
1/f^2

Figure(s)

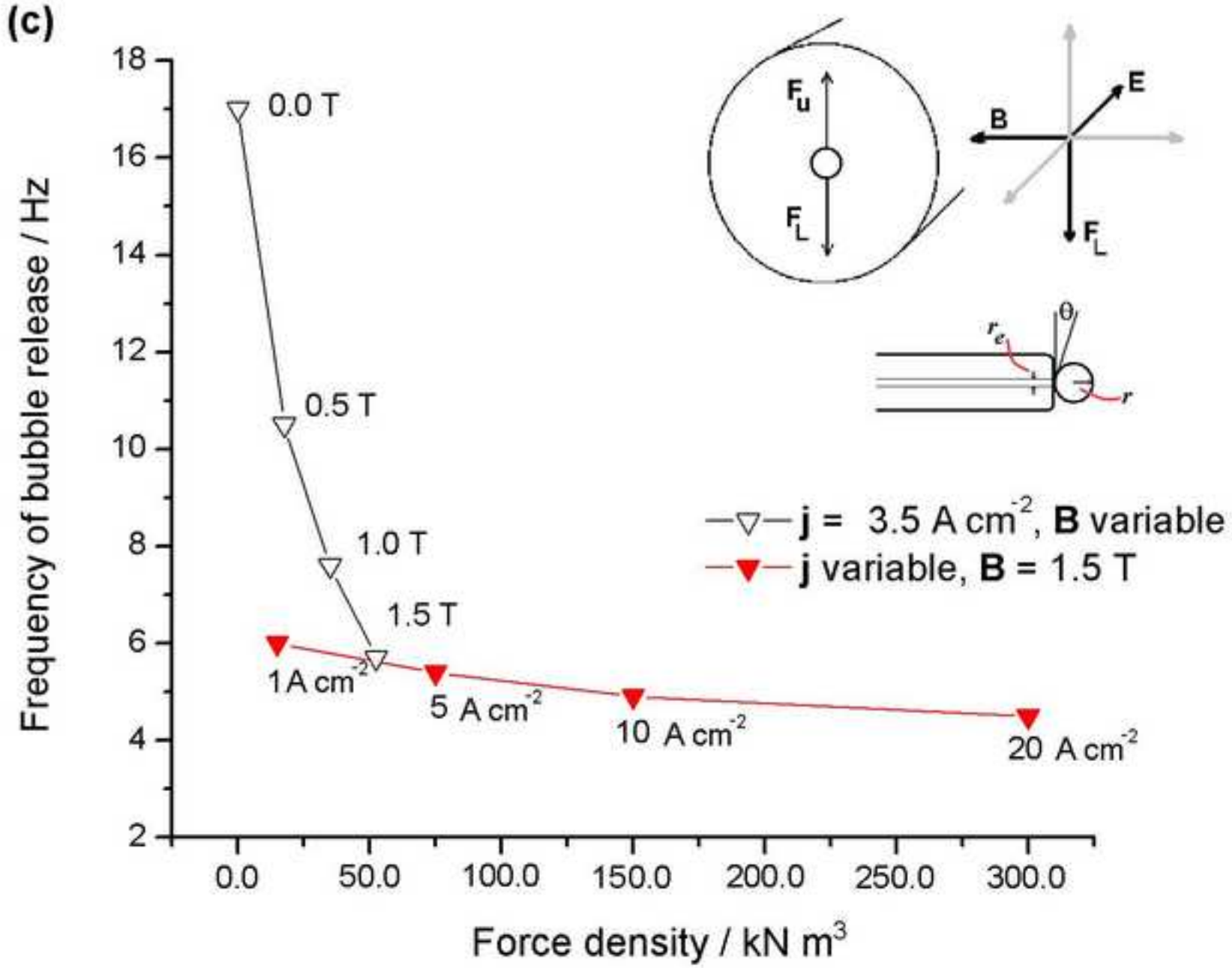
(c)
Frequency of bubble release / Hz
Force density / kN m3
0.0 T
0.5 T
1.0 T
1.5 T
1A cm-2
5 A cm-2
10 A cm-2
20 A cm-2
j = 3.5 A cm-2, B variable
j variable, B = 1.5 T
Fu
FL
B
E
FL
θ
re
r

Figure(s)

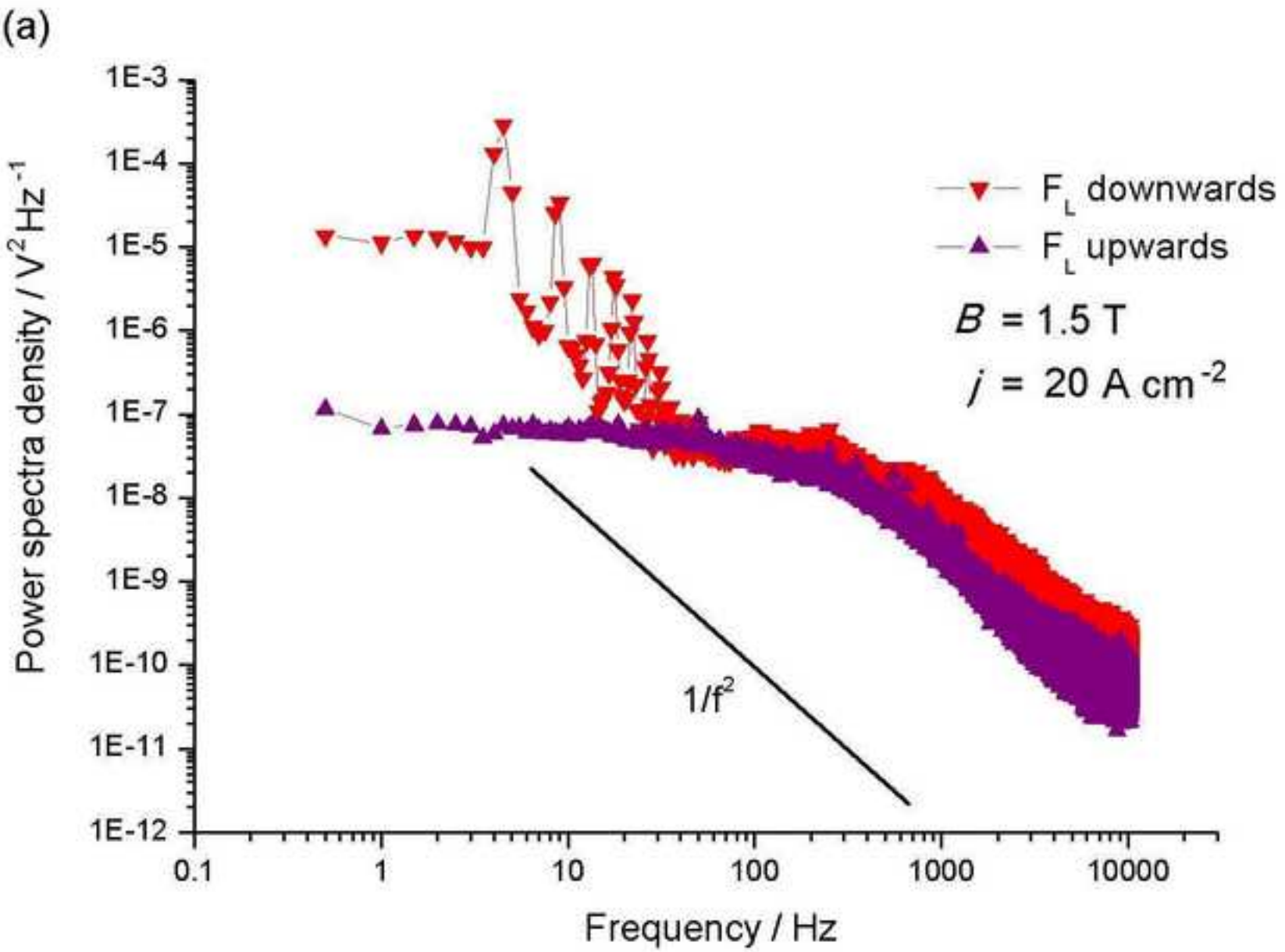
(a)
Power spectra density / V^{2}Hz^{-1}
1E-3
1E-4
1E-5
1E-6
1E-7
1E-8
1E-9
1E-10
1E-11
1E-12
0.1
1
10
100
1000
10000
Frequency / Hz
F$_L$ downwards
F$_L$ upwards
B = 1.5 T
j = 20 A cm^{-2}
1/f^2

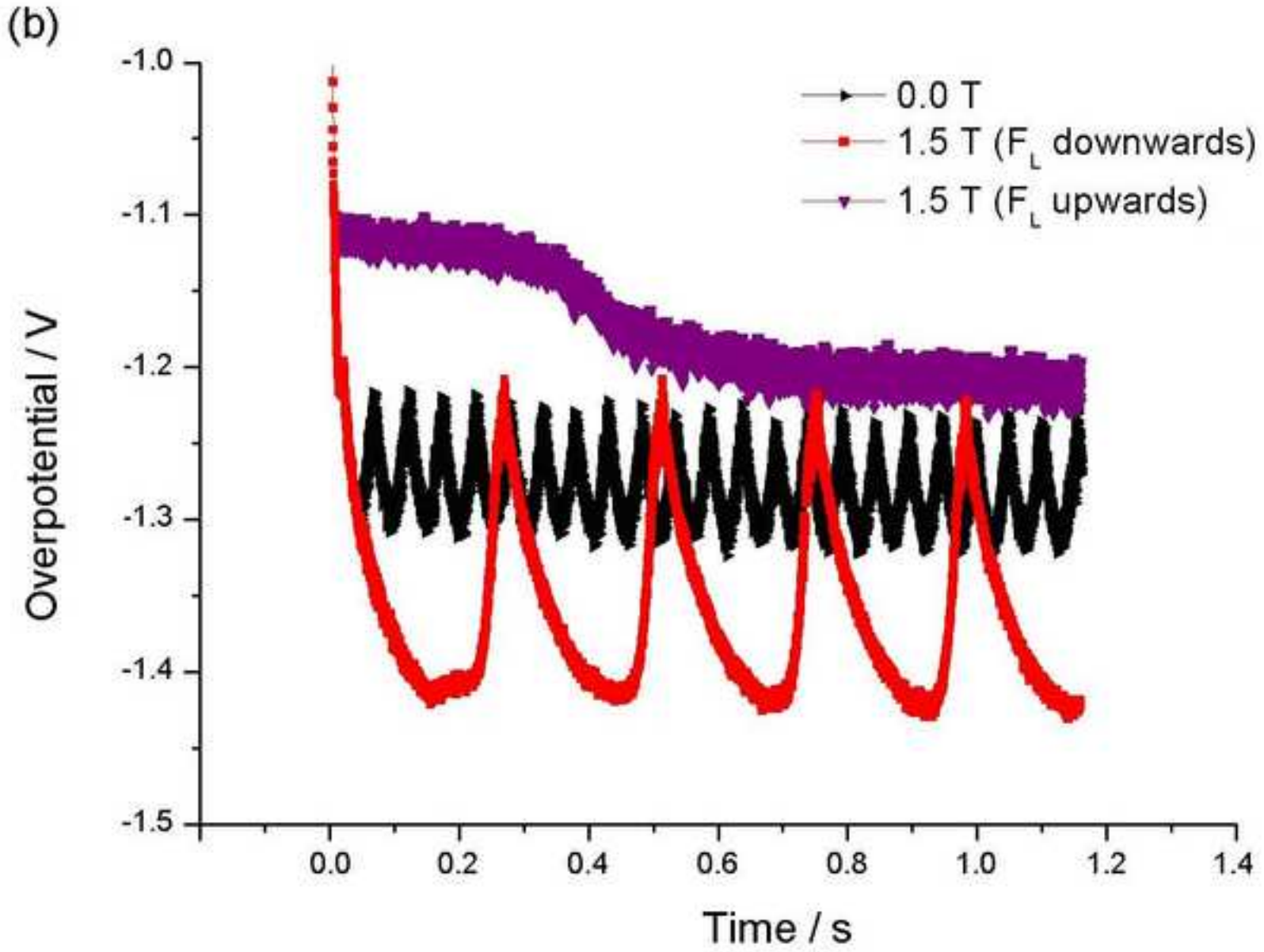
(b)
-1.0
-1.1
-1.2
-1.3
-1.4
-1.5
Overpotential / V
0.0
0.2
0.4
0.6
0.8
1.0
1.2
1.4
Time / s
0.0 T
1.5 T (F_L downwards)
1.5 T (F_L upwards)

Figure(s)

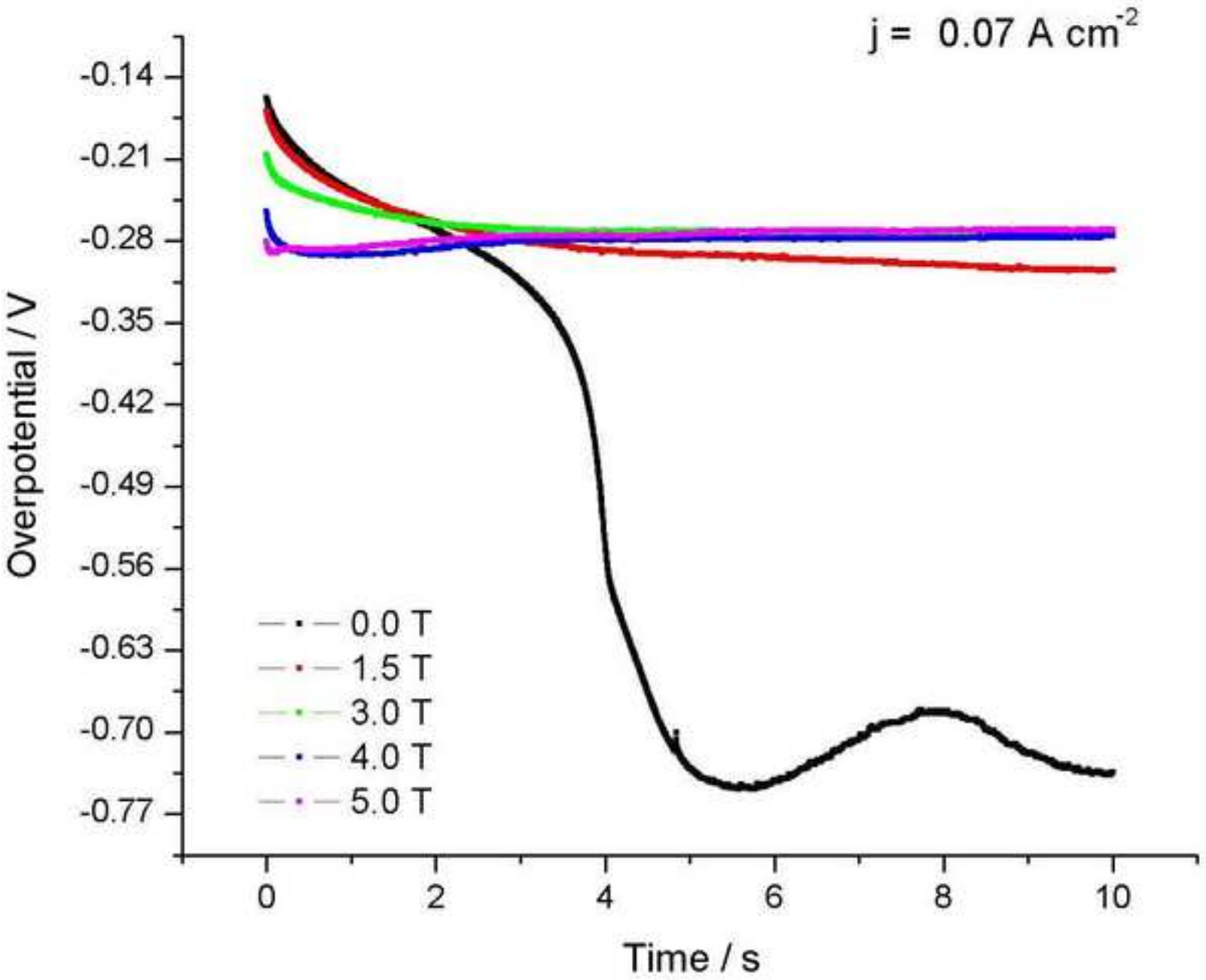
j = 0.07 A cm-2
Overpotential / V
-0.14
-0.21
-0.28
-0.35
-0.42
-0.49
-0.56
-0.63
-0.70
-0.77
0.0 T
1.5 T
3.0 T
4.0 T
5.0 T
0
2
4
6
8
10
Time / s

Figure(s)

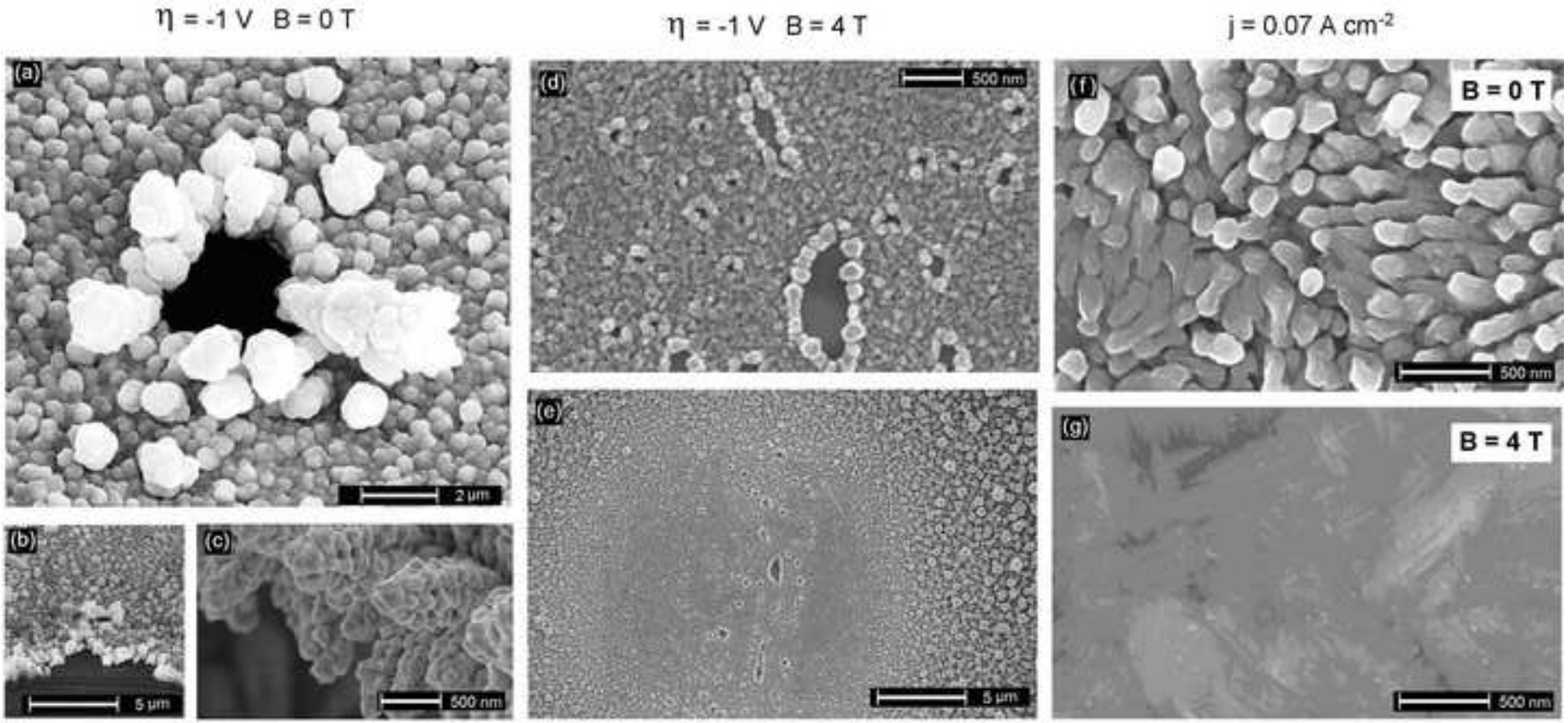
η = -1 V B = 0 T
η = -1 V B = 4 T
j = 0.07 A cm-2
(a)
2 µm
(b)
5 µm
(c)
500 nm
(d)
500 nm
(e)
5 µm
(f)
B = 0 T
500 nm
(g)
B = 4 T
500 nm

Figure(s)

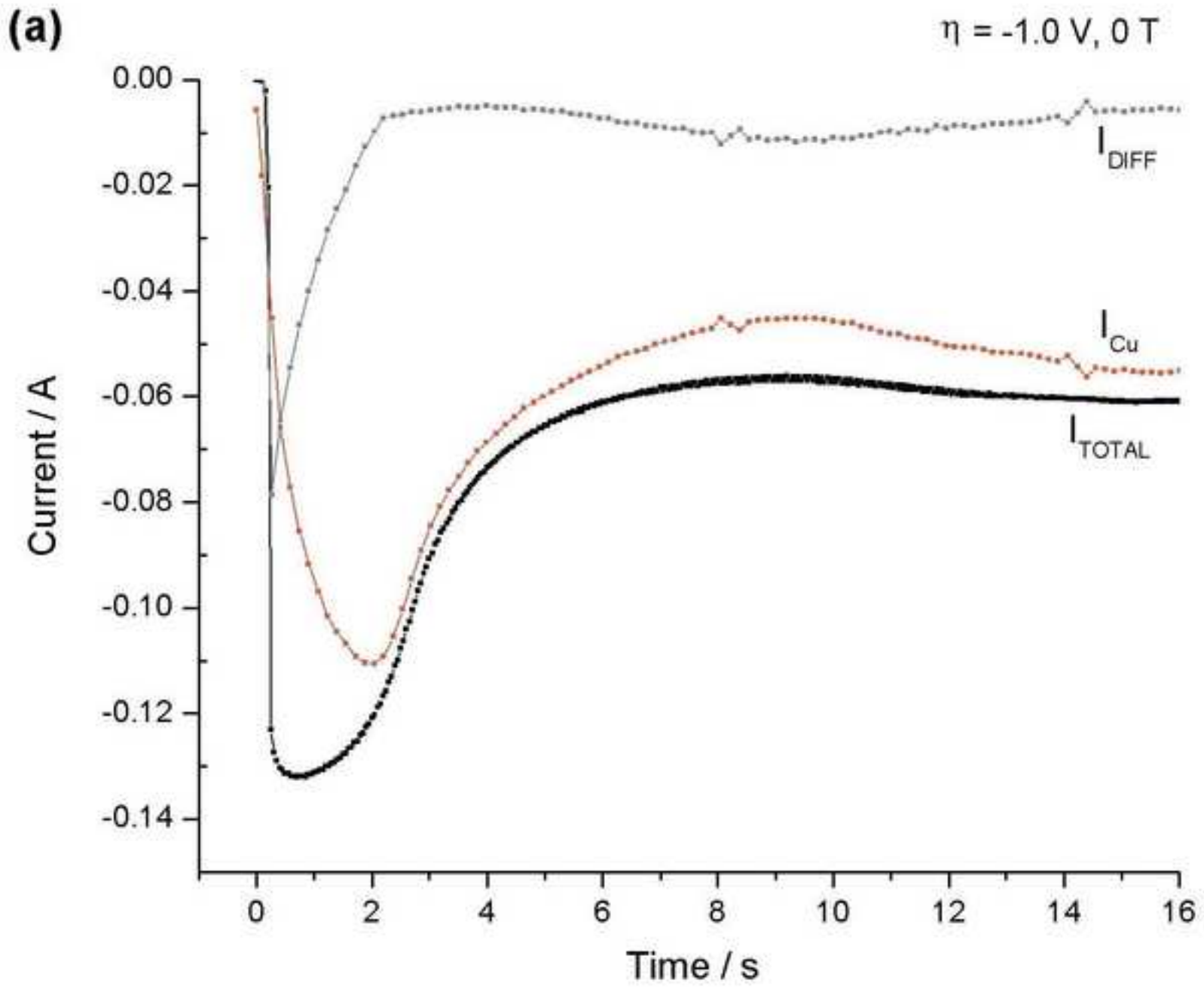
(a)
η = -1.0 V, 0 T
0.00
-0.02
-0.04
-0.06
-0.08
-0.10
-0.12
-0.14
Current / A
0
2
4
6
8
10
12
14
16
Time / s
I DIFF
I Cu
I TOTAL

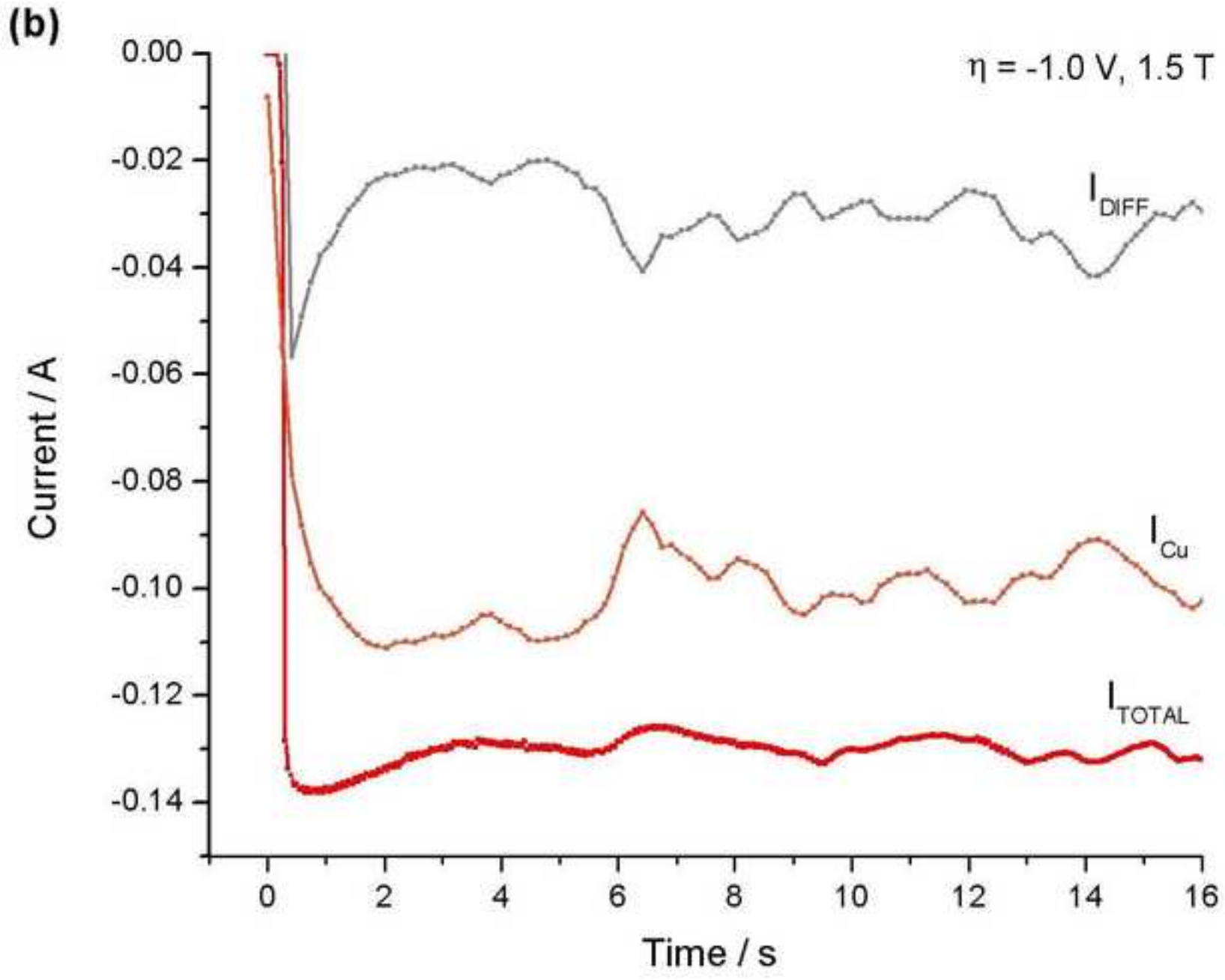
(b)
η = -1.0 V, 1.5 T
I DIFF
I Cu
I TOTAL
Current / A
Time / s
0.00
-0.02
-0.04
-0.06
-0.08
-0.10
-0.12
-0.14
0
2
4
6
8
10
12
14
16

Figure(s)

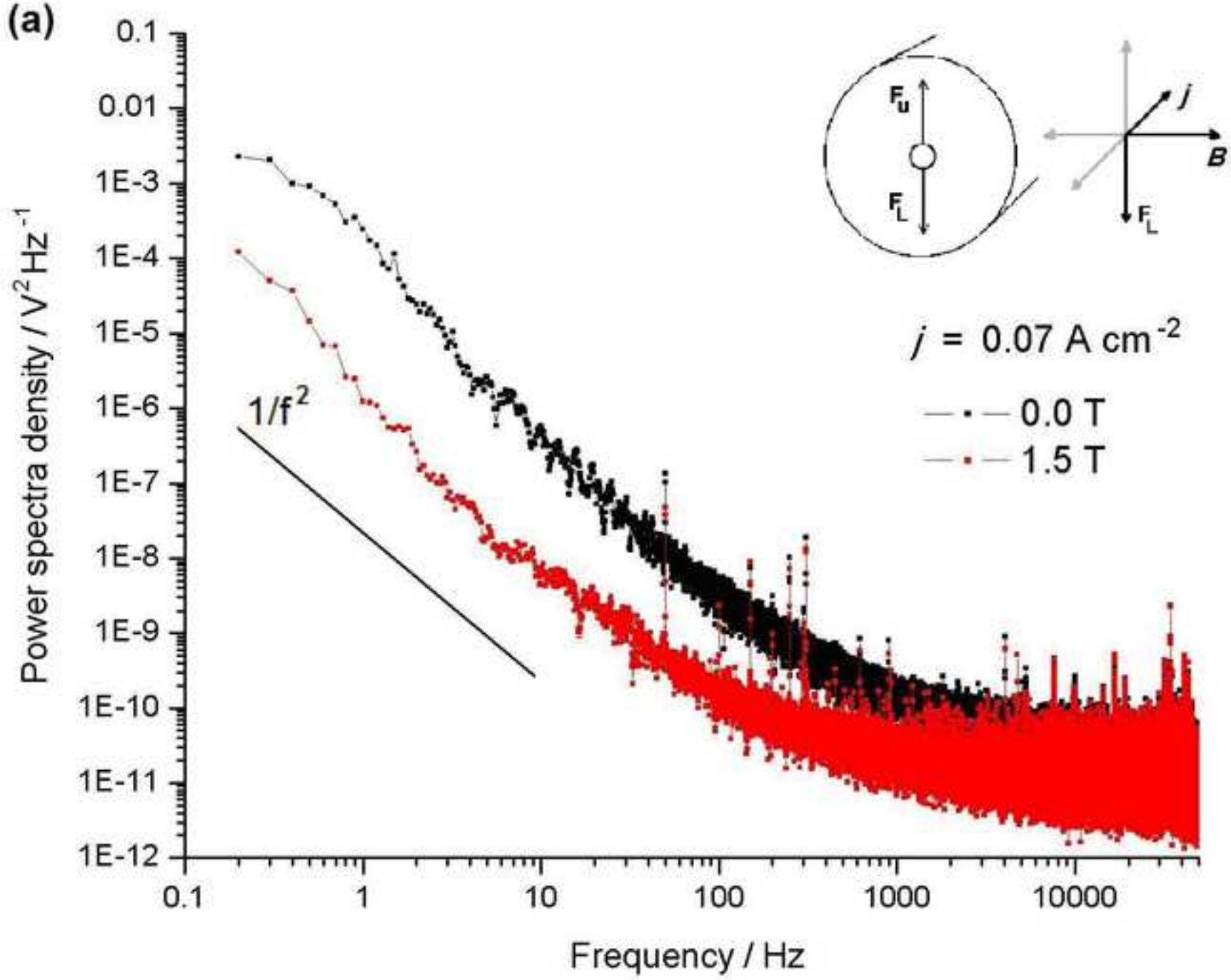
(a)
Power spectra density / V² Hz⁻¹
0.1
0.01
1E-3
1E-4
1E-5
1E-6
1E-7
1E-8
1E-9
1E-10
1E-11
1E-12
1/f²
j = 0.07 A cm⁻²
0.0 T
1.5 T
F_u
F_L
j
B
F_L
0.1
1
10
100
1000
10000
Frequency / Hz

Figure(s)

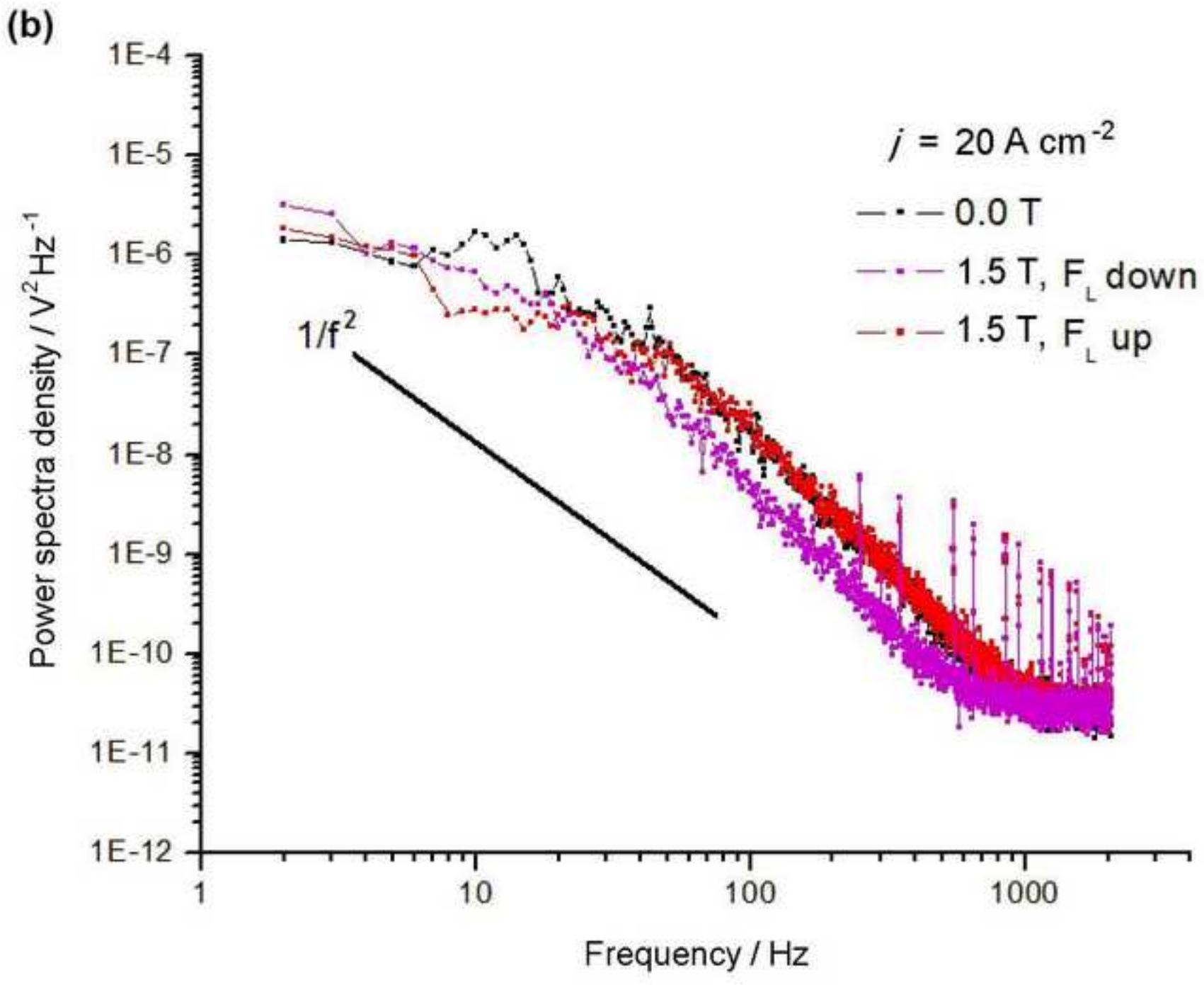
(b)
1E-4
1E-5
1E-6
1E-7
1E-8
1E-9
1E-10
1E-11
1E-12
Power spectra density / V^{2}Hz^{-1}
1/f^2
j = 20 A cm^{-2}
0.0 T
1.5 T, F$_L$ down
1.5 T, F$_L$ up
1
10
100
1000
Frequency / Hz